



Synthesis, structure, and optical properties of $\text{CsU}_2(\text{PO}_4)_3$

George N. Oh, Emilie Ringe, Richard P. Van Duyne, James A. Ibers*

Department of Chemistry, Northwestern University, 2145 Sheridan Road, Evanston, IL 60208-3113, USA

ARTICLE INFO

Article history:

Received 6 September 2011

Received in revised form

4 October 2011

Accepted 4 October 2011

Available online 11 November 2011

Keywords:

Cesium diuranium triphosphate

Single-crystal X-ray structure

Optical absorption measurements

Pleochroism

ABSTRACT

$\text{CsU}_2(\text{PO}_4)_3$ was synthesized in highest yield by the reaction in a fused-silica tube of U, P, and Se in a CsCl flux at 1273 K. It crystallizes with four formula units in space group $P2_1/n$ of the monoclinic system in a new structure type. The structure of $\text{CsU}_2(\text{PO}_4)_3$ is composed of U and Cs atoms coordinated by PO_4^{3-} units in distorted octahedral arrangements. Each U atom corner shares with six PO_4^{3-} units. Each Cs atom face shares with one, edge shares with two, and corner shares with three PO_4^{3-} units. The structure shares some features with the sodium zirconium phosphate structure type. X-ray powder diffraction results demonstrate that the present $\text{CsU}_2(\text{PO}_4)_3$ compound crystallizes in a structure different from the previously reported β' - and γ - $\text{CsU}_2(\text{PO}_4)_3$ compounds. $\text{CsU}_2(\text{PO}_4)_3$ is highly pleochroic, as demonstrated by single-crystal optical absorption measurements.

© 2011 Elsevier Inc. All rights reserved.

1. Introduction

Crystalline phosphate compounds have been studied for their potential as a mineral-like matrix for immobilizing actinides found in high-level nuclear waste. Such phosphates include monazites, thorium phosphates, and apatites [1–6]. Phosphates in particular are of interest owing to their thermal stability [7] and geochemical stability [8]. Many naturally-occurring tetravalent uranium compounds occur as phosphates [9]. These compounds crystallize in a variety of structure types [10]. Such structure types can incorporate early actinides, lanthanides, alkali metals, and alkaline-earth metals [11]. Mixed-metal phosphates have also been synthesized, which demonstrates their ability to incorporate a number of elements simultaneously [12]. A class of compounds in this family are those with formula $AAn_2(\text{PO}_4)_3$ (A =alkali metal, An =actinide) [10,11,13]. Two structure types are common for this class: the $\text{NaTh}_2(\text{PO}_4)_3$ or NTP structure type, and the kosnarite ($\text{KZr}_2(\text{PO}_4)_3$) or NZP structure type [14]. These structures are in space groups $C2/c$ and $R\bar{3}c$, respectively, and have been labeled α - and β - $AAn_2(\text{PO}_4)_3$ [13]. All of the Th compounds crystallize in the NTP structure type [11]. The following actinide compounds also crystallize in this structure type: $\text{LiU}_2(\text{PO}_4)_3$ and $\text{NaU}_2(\text{PO}_4)_3$ [11], $\text{KU}_2(\text{PO}_4)_3$ [15], $\text{RbNp}_2(\text{PO}_4)_3$, $\text{NaPu}_2(\text{PO}_4)_3$ [16], and $\text{KPu}_2(\text{PO}_4)_3$ [13]. Compounds that crystallize in the NZP structure type include $AAn_2(\text{PO}_4)_3$ (A =Na, K, Rb; An =U, Np, Pu) [17,18] and $\text{CsNp}_2(\text{PO}_4)_3$ [13]. Some of these compounds crystallize in both structure types, and phase transitions have been observed between them, with the NZP structure type formed at higher temperatures.

Additional phases have been identified from X-ray powder diffraction experiments [13].

Compounds with the NZP structure type have also shown some ability to immobilize alkali metals via ion exchange. For instance, $\text{HZr}_2(\text{PO}_4)_3$ immobilizes Cs via ion exchange [19]. In some cases, the cations are not immobilized, especially when they are small and the cavities are enlarged. For example, in $\text{LiZr}_2(\text{P}_{0.33}\text{Si}_{0.66}\text{O}_4)_3$ the substitution of Si for P enlarges the cavities such that Li is mobile [20]. Such compounds are used as ionic conductors, and in this context are referred to as NASICON-type compounds [21]. Two phases have been reported for $\text{CsU}_2(\text{PO}_4)_3$, β' and γ [13]. Powder patterns were reported for both, but neither of their structures was determined. Here we report the synthesis and crystal structure of cesium diuranium triphosphate, $\text{CsU}_2(\text{PO}_4)_3$. We examine its structural features and compare them to the NZP structure type. We also report the optical absorption spectrum of this highly pleochroic compound.

2. Experimental

2.1. Synthesis

All reactants except UO_2 and Se were handled in an argon-filled glove box. UP_2 powder was synthesized by the stoichiometric reaction of U turnings (Oak Ridge National Laboratory) with red P (Alfa Aesar, 99%). The mixture was placed in a 9 mm outer-diameter carbon-coated fused-silica tube and flame-sealed under 10^{-4} Torr vacuum. It was then placed in a computer-controlled furnace and heated to 1273 K in 24 h, held for 96 h, cooled to 773 K in 99 h, to 473 K in 30 h, and to 298 K in 12 h. UO_2 was synthesized by following a previously reported

* Corresponding author. Fax: +1 8474912976.

E-mail address: ibers@chem.northwestern.edu (J.A. Ibers).

procedure [22]: UO_3 (Kerr–McGee Nuclear Corp) was heated to 1173 K, then cooled to 298 K, all under H_2 flow. Se (Cerac, 99.999%), CsCl (MP, Optical grade 99.9%), SiO_2 (Aldrich), and P_2O_5 (Mallinckrodt, 99.5%) were used as received.

$\text{CsU}_2(\text{PO}_4)_3$ was synthesized by combining UP_2 (0.100 mmol), Se (0.100 mmol), and CsCl (0.891 mmol) in a 6 mm carbon-coated fused-silica tube. The tube was sealed, and heated to 1273 K in 24 h, held for 192 h, cooled to 1223 K in 24 h, held for 192 h, cooled to 823 K in 120 h, then to 298 K in 24 h. The ampule emerged somewhat etched, and washing the contents in water afforded highly faceted crystals of $\text{CsU}_2(\text{PO}_4)_3$ in roughly 20 wt% yield together with green–black crystals of U_3O_8 and black crystals of USe_2 . The crystals of $\text{CsU}_2(\text{PO}_4)_3$ are highly pleochroic, appearing lavender or teal, depending on the direction from which they are viewed. The color change can also be observed under polarized light (Fig. 1). The crystals are air-stable. Qualitative EDS-enabled SEM analysis on single crystals indicated the presence of Cs, U, P, and O, but not of Se. The oxygen source in this reaction was the silica tube. Attempts at rational syntheses of $\text{CsU}_2(\text{PO}_4)_3$ using UO_2 , P_2O_5 , with or without additional oxygen sources such as SiO_2 , generated the compound in lower yields. $\alpha\text{-UP}_2\text{O}_7$ was the major product in these reactions [23].

2.2. Structure determination

Single-crystal X-ray diffraction data were collected on a Bruker KAPPA diffractometer with an APEXII CCD detector with the use of Mo $K\alpha$ radiation ($\lambda=0.71073$ Å). A data collection strategy consisting of ϕ and ω scans was devised using COSMO in APEX2 [24]. The data frames were 0.3° in width and taken at a detector distance of 60 mm with exposure times of 15 s/frame. Examination of the data showed that the crystal was twinned by pseudomerohedry, with the second domain rotated 180° about the b axis. Initial cell refinement and data reduction were carried out with SAINT in APEX2 [24]. The structure was solved with XS and refined with XL of the SHELX package [25]. The data were reintegrated with a second domain, related to the first by the twin law $-1\ 0\ 0\ 0\ 1\ 0\ 0\ 0\ -1$, then corrected for absorption with TWINABS [26]. A satisfactory solution was obtained with 19.8(1)% of the crystal in the second domain. Additional crystallographic details are given in Table 1 and the Supporting material, and selected metrical details are given in Table 2.

2.3. Powder X-ray diffraction measurements

The powder diffraction pattern of the present $\text{CsU}_2(\text{PO}_4)_3$ compound was obtained in order to compare it to those previously reported for β' - and γ - $\text{CsU}_2(\text{PO}_4)_3$ [13]. Single crystals were ground and then analyzed with a Rigaku Geigerflex X-ray powder diffractometer with the use of $\text{CuK}\alpha$ radiation ($\lambda=1.5418$ Å). The sample was scanned in the range $2\theta=5\text{--}35^\circ$.

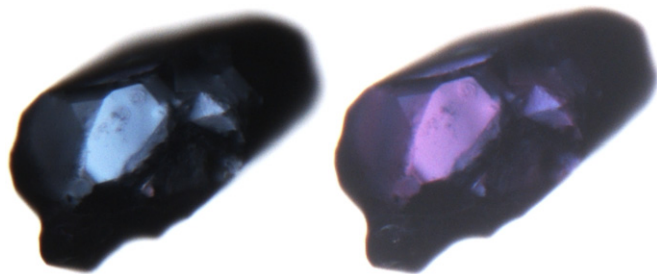


Fig. 1. A $\text{CsU}_2(\text{PO}_4)_3$ crystal viewed through polarized light. The polarizer was rotated approximately 90° between the views. (For interpretation of the references to color in this figure, the reader is referred to the web version of this article.)

Table 1
Crystallographic details for $\text{CsU}_2(\text{PO}_4)_3$.

Formula mass	893.88
Space group	$C_{2h}^5\text{-}P2_1/n$
a (Å)	9.2136(4)
b (Å)	8.6548(3)
c (Å)	15.0161(6)
β (deg.)	91.240(2)
V (Å ³)	1197.13
ρ_c (g cm ⁻³)	4.960
T (K)	100(2)
Z	4
μ (mm ⁻¹)	30.47 (Mo $K\alpha$)
$R(F)^a$	0.0199
$R_w(F^2)^b$	0.0525

$$^a R(F) = \frac{\sum \|F_o\| - |F_c|}{\sum \|F_o\|} \text{ for } F_o^2 > 2\sigma(F_o^2).$$

$$^b R_w(F^2) = \frac{(\sum wF_o^2 - F_c^2)^2 / \sum wF_o^4}{\sum wF_o^4}^{1/2}. \text{ For } F_o^2 < 0, w^{-1} = \sigma^2(F_o^2); \text{ For } F_o^2 \geq 0, w^{-1} = \sigma^2(F_o^2) + (0.0243F_o^2)^2.$$

Table 2
Selected Interatomic distances (Å) and angles (deg.) for $\text{CsU}_2(\text{PO}_4)_3$.

U1–O9	2.223(4)	O9–U1–O5	92.2(1)
U1–O5	2.224(3)	O5–U1–O11	100.1(1)
U1–O11	2.250(4)	O9–U1–O8	88.1(1)
U1–O8	2.265(4)	O9–U1–O3	77.3(1)
U1–O3	2.318(4)	O9–U1–O4	84.1(1)
U1–O4	2.327(4)	O9–U1–O4	110.6(1)
U1–O4	2.793(4)	O1–U2–O7	83.8(1)
U2–O1	2.198(3)	O1–U2–O12	90.7(1)
U2–O7	2.214(4)	O12–U2–O10	98.0(1)
U2–O12	2.225(4)	O1–U2–O6	90.2(1)
U2–O10	2.241(4)	O1–U2–O2	95.1(1)
U2–O6	2.255(4)		
U2–O2	2.268(4)		

Scan times were 20 s, with 0.02° steps between scans. The spectrum was calibrated by an internal Si standard with the use of JADE8 [27]. A simulated powder pattern was generated from the single-crystal data with the use of PLATON [28].

2.4. Optical measurements

Single-crystal optical absorption measurements were performed over the range from 3.2 eV (387 nm) to 1.5 eV (827 nm) at room temperature. A single crystal of $\text{CsU}_2(\text{PO}_4)_3$ mounted on a goniometer head was attached to a custom-made holder fitted to a Nikon Eclipse Ti2000–U inverted microscope. The crystal was positioned at the focal plane of the microscope and illuminated with a polarization-filtered tungsten–halogen lamp. The transmitted light was spatially filtered with a $200\ \mu\text{m}$ aperture, dispersed by a 150 groove/mm grating in an Acton SP2300 imaging spectrometer, and collected on a back-illuminated, liquid nitrogen-cooled CCD (Spec10:400BR, Princeton Instruments). Spectra were taken at 10° increments of the polarizer angle.

3. Results and discussion

3.1. Synthesis

$\text{CsU}_2(\text{PO}_4)_3$ was synthesized initially in approximately 20 wt% yield from the reaction in a fused-silica tube of UP_2 with Se in a CsCl flux. The other products were U_3O_8 and USe_2 in about equal amounts. Subsequent reactions using P_2O_5 afforded primarily purple crystals of UP_2O_7 and only a few crystals of $\text{CsU}_2(\text{PO}_4)_3$. Reactions utilizing UO_2 did not provide any green–black crystals of U_3O_8 , which is unusual considering the oxophilicity of U.

The role of Se is not well understood, but such spectator elements frequently aid the synthesis of chalcogenide compounds, such as U in the synthesis of CsTi_5Te_8 [29].

3.2. Structure

The crystal structure of $\text{CsU}_2(\text{PO}_4)_3$ is composed of U and Cs atoms coordinated by PO_4^{3-} units in distorted octahedral arrangements. In the structure there are two crystallographically independent U atoms. Atom U1 corner shares with six PO_4^{3-} units, with one additional longer distance to another O atom. Atom U2 corner shares with six PO_4^{3-} units. Atom Cs1 face shares with one, edge shares with two, and corner shares with the remaining three PO_4^{3-} units (Fig. 2). Charge balance may be achieved by assigning formal cationic oxidation states as Cs (I), U (IV), and P (V).

Interatomic distances are typical for the coordination numbers and valencies of U and Cs: U1–O distances are in the range of 2.223(4)–2.327(4) Å with an additional long distance at 2.793(4) Å, similar to that found in $\text{U}(\text{UO}_2)(\text{PO}_4)_2$, 2.158–2.604 Å [30]. U2–O distances range from 2.198(4) Å to 2.268(4) Å, smaller than in $\text{KU}_2(\text{PO}_4)_3$, 2.269–2.320 Å [18]. Cs–O distances range from 3.019(4) Å to 3.592(4) Å. These values are within the range of 2.949–3.733 Å found in Cs_2MoO_4 [31].

The overall structure may be visualized by dividing it into layers parallel to (010). The triangular faces of the UO_6 distorted octahedra are approximately aligned to the plane of the layer. These octahedra sit on the corners of a band of double triangles two UO_6 octahedra wide. P1 and P2 tetrahedra sit above and below the triangles, corner sharing with three adjacent UO_6 octahedra. P3 tetrahedra corner share with two UO_6 octahedra at the edge of this band. Each Cs atom lies between these bands in a zig-zag pattern, corner sharing with one of its symmetry-related equivalents (Fig. 3). The layers are stacked along [010] such that the Cs atoms in the next layer are coordinated to the last vertices

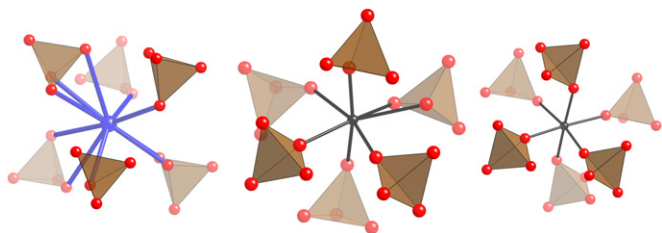


Fig. 2. Coordination environments for atoms U1, U2, and Cs1. U is black, Cs is blue, O is red, and PO_4^{3-} tetrahedra are brown. (For interpretation of the references to color in this figure legend, the reader is referred to the web version of this article.)

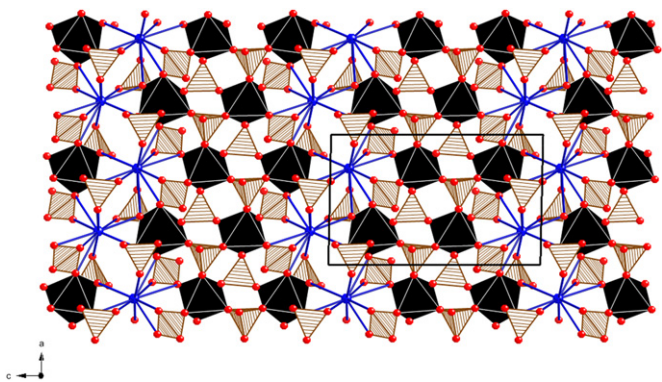


Fig. 3. A single layer of the $\text{CsU}_2(\text{PO}_4)_3$ structure viewed down [010]. U octahedra are black, Cs atoms are blue, and PO_4^{3-} tetrahedra are striped brown. (For interpretation of the references to color in this figure legend, the reader is referred to the web version of this article.)

of the PO_4^{3-} tetrahedra sitting on the triangles of the adjacent layer (Fig. 4).

This structure is related to the NZP structure type, in which $\beta\text{-KU}_2(\text{PO}_4)_3$ crystallizes. $\beta\text{-KU}_2(\text{PO}_4)_3$ is composed of a triangular network of corner-sharing UO_6 octahedra and PO_4^{3-} tetrahedra, in this case parallel to (001). Unlike $\text{CsU}_2(\text{PO}_4)_3$, the alkali metal is also six-coordinate, so instead of bands of UO_6 octahedra separated by Cs atoms, the UO_6 octahedra are in a hexagonal arrangement with the K atoms in the middle of the hexagon (Fig. 5). The layers are stacked with the K atoms on three corners of the hexagon above it, in an *abcabc* stacking arrangement (Fig. 6), resulting in a framework structure. Cs is not stable in this small coordination environment. The high temperature of the present reaction favors the thermodynamically stable product, which contains Cs atoms in a larger coordination environment.

One factor relevant to the immobilizing power of $\text{CsU}_2(\text{PO}_4)_3$ is the strength of the U–O bonds. Shorter interatomic distances correspond to greater bond strength. As noted earlier, the interatomic U–O distances in $\text{CsU}_2(\text{PO}_4)_3$ and $\beta\text{-KU}_2(\text{PO}_4)_3$ are similar, as are the coordination environments. $\beta\text{-KU}_2(\text{PO}_4)_3$ effectively immobilizes U; this suggests that $\text{CsU}_2(\text{PO}_4)_3$ might also be able to do so.

Mobility of alkali metals is more closely linked to the presence of structural motifs such as channels and layers. There are small channels in the $\text{CsU}_2(\text{PO}_4)_3$ structure (Fig. 3). Ionic mobility in channel structures may be estimated from the channel size Δ , where Δ is equal to the shortest open distance between two atoms on opposite sides of the channel measured perpendicular

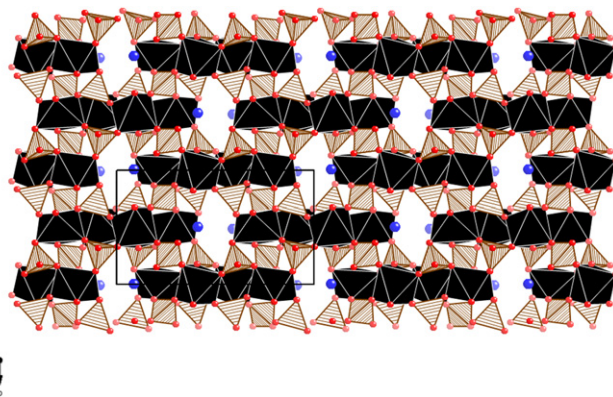


Fig. 4. Stacking of the layers in $\text{CsU}_2(\text{PO}_4)_3$, viewed along [100]. Cs–O bonds are omitted.

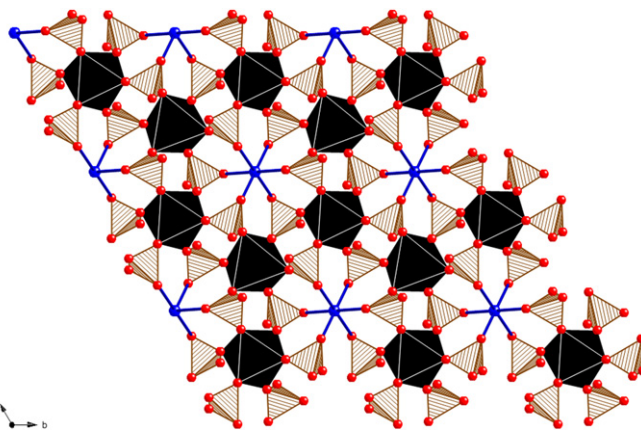


Fig. 5. A single layer of the NZP structure type viewed down [001]. U octahedra are black, K atoms are blue, and PO_4^{3-} tetrahedra are striped brown. (For interpretation of the references to color in this figure legend, the reader is referred to the web version of this article.)

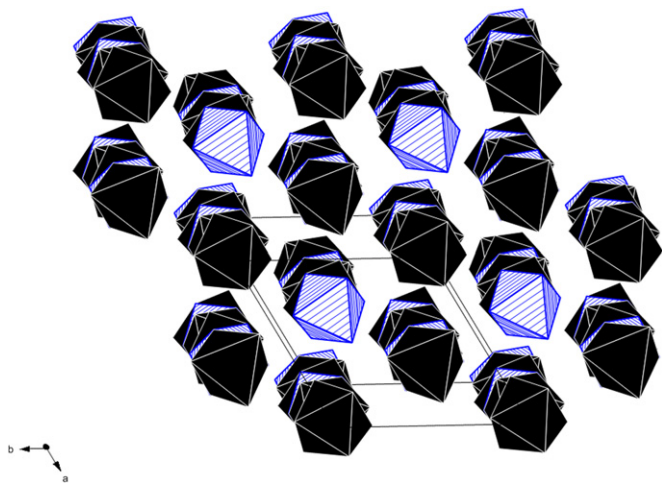


Fig. 6. *abcabc* stacking arrangement in NZP, viewed down [001]. U octahedra are black and K octahedra are striped blue. PO_4^{3-} tetrahedra are omitted. (For interpretation of the references to color in this figure legend, the reader is referred to the web version of this article.)

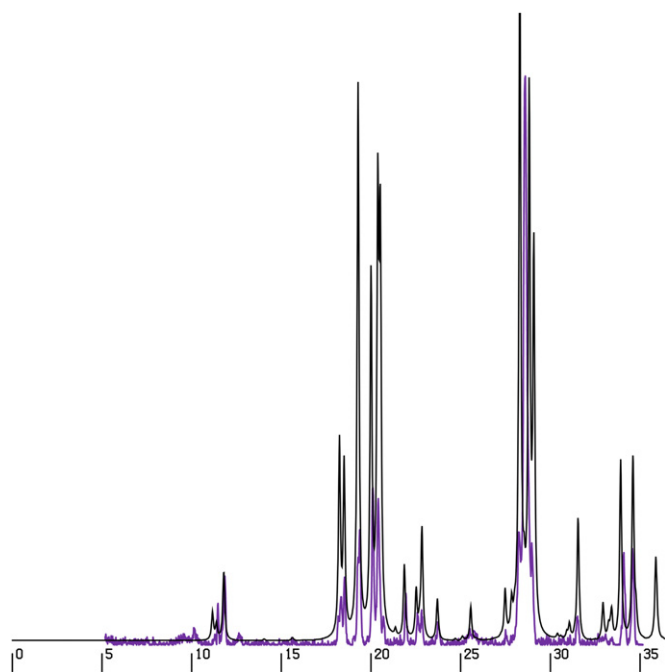


Fig. 7. Simulated powder pattern (black) compared to the experimental powder pattern of $\text{CsU}_2(\text{PO}_4)_3$. Here and in Fig. 8 values of 2θ (CuK α) are along the abscissa. Peak at $2\theta=28.44^\circ$ is from the Si internal standard.

to the channel axis. In the present structure, the shortest interatomic distance of $4.39(1)$ Å is between atom O8 and one of its symmetry equivalents. Subtraction of the crystal radii for both O^{2-} atoms from this distance leaves an open distance of $1.97(2)$ Å, significantly smaller than the crystal diameter of ten-coordinate Cs, 3.9 Å [32]. Any movement of Cs in $\text{CsU}_2(\text{PO}_4)_3$ would require a large deformation of the structure, suggesting U and Cs might both be immobile in $\text{CsU}_2(\text{PO}_4)_3$. Note that the NZP-type $\text{CsZr}_2(\text{PO}_4)_3$ has been shown to be an effective immobilization matrix for Cs and it has a much larger Δ of $3.69(2)$ Å [19].

3.3. Comparison to β' - and γ - $\text{CsU}_2(\text{PO}_4)_3$

An experimental powder pattern as well as one simulated from the single-crystal data of $\text{CsU}_2(\text{PO}_4)_3$ is compared in

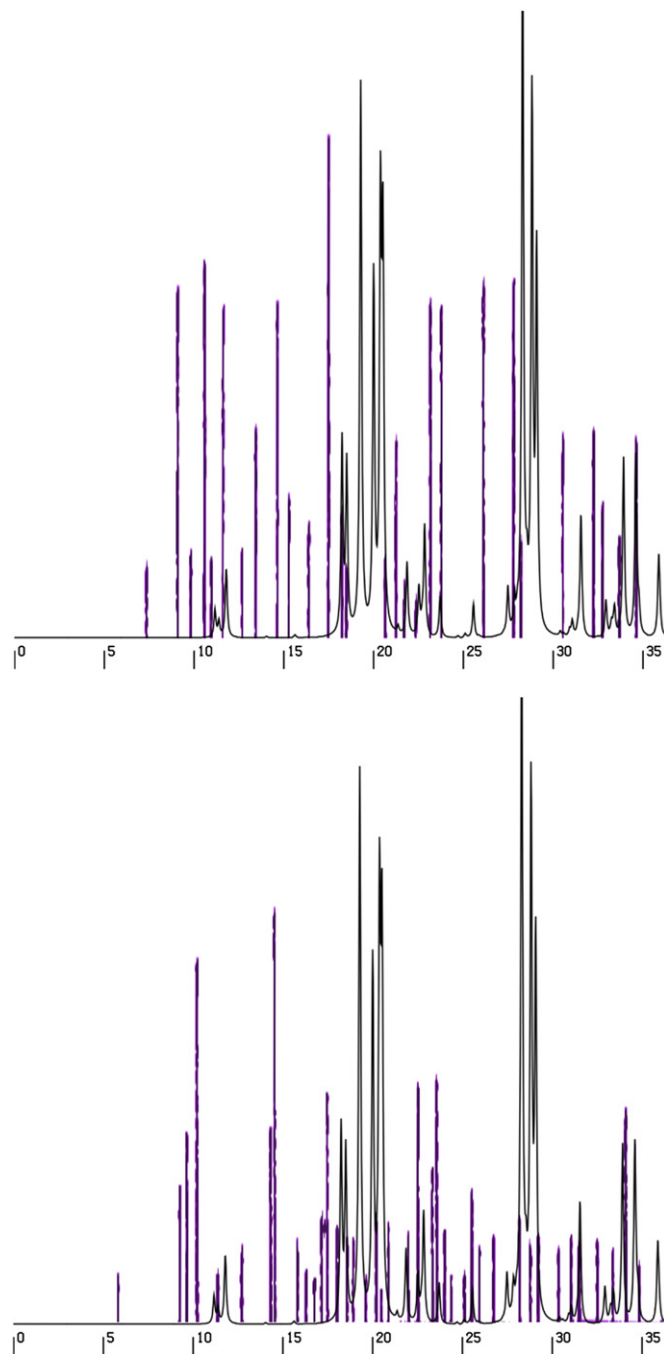


Fig. 8. Simulated powder pattern (black) compared to the previously reported (β' - (top) and γ - $\text{CsU}_2(\text{PO}_4)_3$ (bottom) patterns. (For interpretation of the references to color in this figure legend, the reader is referred to the web version of this article.)

Figs. 7 and 8 with those previously reported for β' - and γ - $\text{CsU}_2(\text{PO}_4)_3$ [13]. Our experimental powder pattern is in good agreement with the simulated powder pattern, but those for both β' and γ phases are in poor agreement, in part because they display many low-angle peaks that do not appear on the simulated pattern. The presence of impurities would not account for the overall poor agreement between the simulated and those experimental powder patterns. From these comparisons we conclude that the structure presented here is new, being neither that of β' - nor that of γ - $\text{CsU}_2(\text{PO}_4)_3$.

Whereas the reaction temperature for the synthesis of the present $\text{CsU}_2(\text{PO}_4)_3$ is in the range used to synthesize

β' - $\text{CsU}_2(\text{PO}_4)_3$, the overall synthetic route is completely different. The previously reported compounds were synthesized by reacting UO_2 , CsNO_3 , and 1 M H_3PO_4 at 373–573 K, then annealing under an Ar atmosphere between 1173 K and 1373 K for β' - $\text{CsU}_2(\text{PO}_4)_3$, and between 1373 and 1773 K for γ - $\text{CsU}_2(\text{PO}_4)_3$.

3.4. Optical properties

The transmittance spectra of $\text{CsU}_2(\text{PO}_4)_3$ are presented in Fig. 9. The peaks are sharp and fairly weak, typical of f - f transitions [33]. Such transitions are between states split by the crystal field of the U atoms [34]. Weak pleochroism is a common property of colored solid-state compounds [35]. $\text{CsU}_2(\text{PO}_4)_3$ exhibits strong pleochroism, which is much rarer but is found in minerals such as tourmaline, iolite, and andalusite. Structures with orthorhombic or lower symmetry may display trichroism. However, measurements on additional faces of $\text{CsU}_2(\text{PO}_4)_3$ produced similar spectra; thus the compound is dichroic rather than trichroic.

Pleochroism is a result of anisotropy in the coordination environment of optically active atoms. Atom U2 is in a nearly

octahedral coordination environment whereas atom U1 is not and is probably the source of the pleochroism. The f - f transitions most affected by this anisotropy are located around 1.95, 2.07, and 2.26 eV, the latter two being negatively correlated with the first one.

4. Conclusions

We have synthesized and structurally characterized $\text{CsU}_2(\text{PO}_4)_3$, which crystallizes in a new structure type. An X-ray powder diffraction pattern of this compound is not related to the patterns for β' - and γ - $\text{CsU}_2(\text{PO}_4)_3$ that were reported earlier. Examination of the structural features of the present structure suggests that it might be able to immobilize both Cs and U, two important components of nuclear waste. Optical measurements emphasize the importance of crystalline electric field effects in the electronic properties of actinide compounds.

Supporting material

The crystallographic data for $\text{CsU}_2(\text{PO}_4)_3$ has been deposited with FIZ Karlsruhe as CSD number 423508. These data may be obtained free of charge by contacting FIZ Karlsruhe at +497247808666 (fax) or crysdata@fiz-karlsruhe.de (email).

Acknowledgments

Funding for this research was kindly provided by the US Department of Energy, Basic Energy Sciences, Chemical Sciences, Biosciences, and Geosciences Division and Division of Materials Science and Engineering Grant ER-15522, and the National Science Foundation (CHE-0911145) and NSF MRSEC (DMR-0520513) at the Materials Research Center of Northwestern University. SEM analyses were conducted in the Electron Probe Instrumentation Center (EPIC) at the Northwestern University Atomic and Nanoscale Characterization Experimental (NUANCE) Center, supported by NSF-NSEC, NSF-MRSEC, Keck Foundation, the State of Illinois, and Northwestern University. Single-crystal data were collected at the IMSERC X-ray Facility at Northwestern University, supported by the International Institute of Nanotechnology (IIN). Powder X-ray diffraction data were collected at the J. B. Cohen X-Ray Diffraction Facility supported by the MRSEC program of the NSF (DMR-0520513) at the Materials Research Center of Northwestern University.

Appendix A. Supplementary material

Supplementary data associated with this article can be found in the online version at doi:10.1016/j.jssc.2011.10.007.

References

- [1] N. Dacheux, N. Clavier, A.-C. Robisson, O. Terra, F. Audubert, J.-É. Lartigue, C. Guy, C. R. Chimie 7 (2004) 1141–1152.
- [2] O. Terra, N. Dacheux, F. Audubert, R. Podor, J. Nucl. Mater. 352 (2006) 224–232.
- [3] N. Clavier, N. Dacheux, R. Podor, Inorg. Chem. 45 (2006) 220–229.
- [4] L.A. Boatner, Rev. Mineral. Geochem. 48 (2002) 87–121.
- [5] R.C. Ewing, Prog. Nucl. Energy 49 (2007) 635–643.
- [6] N. Clavier, R. Podor, N. Dacheux, J. Eur. Ceram. Soc. 31 (2011) 941–976.
- [7] K. Krishnan, S.K. Sali, K.D. Singh Mudher, J. Alloys Compd. 414 (2006) 310–316.
- [8] T. Murakami, T. Ohnuki, H. Isobe, T. Sato, Am. Mineral. 82 (1997) 888–899.
- [9] I. Grenthe, J. Drozdzyński, T. Fujino, E.C. Buck, T.E. Albrecht-Schmitt, S.F. Wolf, Uranium, in: Third ed., in: L.R. Morss, N.M. Edelstein, J. Fuger (Eds.), The

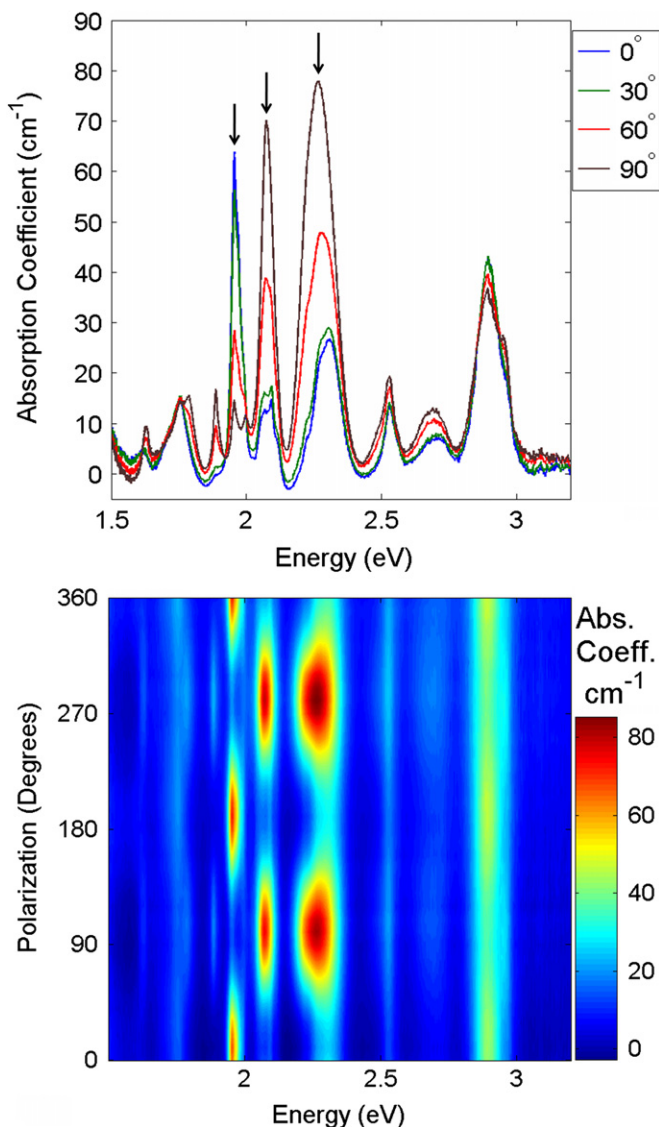


Fig. 9. Absorption coefficient of $\text{CsU}_2(\text{PO}_4)_3$ as a function of energy. The top panel shows polarization from 0 to 90°. Peaks with prominent anisotropy at 1.95, 2.07, and 2.26 eV are marked with arrows. The complete rotation over 360° is presented in the bottom panel.

- Chemistry of the Actinide and Transactinide Elements, vol. 1, Springer, Dordrecht, 2006, pp. 253–698.
- [10] A.J. Locock, *Crystal Chemistry of Actinide Phosphates and Arsenates*, in: 1st ed., in: S.V. Krivovichev, P.C. Burns, I.G. Tananaev (Eds.), *Structural Chemistry of Inorganic Actinide Compounds*, vol. 1, Elsevier, Oxford, 2007, pp. 217–278. (N).
- [11] V. Brandel, N. Dacheux, *J. Solid State Chem.* 177 (2004) 4755–4767.
- [12] Y.F. Volkov, S.V. Tomilin, A.N. Lukinykh, A.A. Lizin, A.I. Orlova, D.B. Kitaev, *Radiochemistry (Transl. of Radiokhimiya)* 44 (2002) 319–325.
- [13] Y.F. Volkov, R.F. Melkaya, V.I. Spiriyakov, G.A. Timofeev, *Radiochemistry (Transl. of Radiokhimiya)* 36 (1994) 222–226.
- [14] M.E. Brownfield, E.E. Foord, S.J. Sutley, T. Botinelly, *Am. Mineral.* 78 (1993) 653–656.
- [15] A. Guesdon, J. Provost, B. Raveau, *J. Mater. Chem.* 9 (1999) 2583–2587.
- [16] A.A. Burnaeva, Y.F. Volkov, A.I. Kryukova, I.A. Korshunov, O.V. Skiba, *Radiochemistry (Transl. of Radiokhimiya)* 34 (1992) 13–21.
- [17] Y.F. Volkov, S.V. Tomilin, A.I. Orlova, A.A. Lizin, V.I. Spiriyakov, A.N. Lukinykh, *Radiochemistry (Transl. of Radiokhimiya)* 45 (2003) 319–328.
- [18] E.R. Gobechiya, Y.K. Kabalov, S.V. Tomilin, A.N. Lukinykh, A.A. Lizin, A.I. Orlova, *Crystallogr. Rep.* 50 (2005) 374–378.
- [19] K. Itoh, S. Nakayama, *J. Mater. Sci.* 37 (2002) 1701–1704.
- [20] A. Clearfield, *Annu. Rev. Mater. Sci.* 14 (1984) 205–229.
- [21] D. Zhu, F. Luo, Z. Xie, W. Zhou, *Rare Metals* 25 (2006) 39–42.
- [22] J.J. Katz, E. Rabinowitch, 1st ed., *The Chemistry of Uranium*, vol. 1, McGraw-Hill, New York, 1951.
- [23] A. Cabeza, M.A.G. Aranda, F.M. Cantero, D. Lozano, M. Martínez-Lara, S. Bruque, *J. Solid State Chem.* 121 (1996) 181–189.
- [24] Bruker, APEX2 Version 2009.5-1 and SAINT Version 7.34a Data Collection and Processing Software, 2009. Bruker Analytical X-Ray Instruments, Inc.: Madison, WI, USA.
- [25] G.M. Sheldrick, *Acta Crystallogr. Sect. A: Found. Crystallogr.* 64 (2008) 112–122.
- [26] G.M. Sheldrick, TWINABS, 2008. University of Göttingen, Göttingen, Germany.
- [27] Materials Data Inc., JADE8, 2007. Livermore, CA.
- [28] A.L. Spek, PLATON, A. Multipurpose Crystallographic Tool, 2008. Utrecht University, Utrecht, The Netherlands.
- [29] D.L. Gray, J.A. Ibers, *J. Alloys Compd.* 440 (2007) 74–77.
- [30] P. Bénard, D. Louër, N. Dacheux, V. Brandel, M. Genet, *Chem. Mater.* 6 (1994) 1049–1058.
- [31] W. Gonschorek, T. Hahn, *Z. Kristallogr.* 138 (1973) 167–176.
- [32] R.D. Shannon, *Acta Crystallogr. Sect. A: Cryst., Phys. Diffr. Theor. Gen. Crystallogr.* 32 (1976) 751–767.
- [33] J.C. Krupa, *J. Alloys Compd.* 225 (1995) 1–10.
- [34] J.C. Krupa, *Inorg. Chim. Acta* 139 (1987) 223–241.
- [35] K. Nassau, 2nd ed., *The Physics and Chemistry of Color: The Fifteen Causes of Color*, vol. 1, Wiley-Interscience, New York, 2001.